Influence of pre-fission particle emission on fragment angular distributions studied for $^{208}Pb(^{16}O,f)$

H. Rossner
Hahn-Meitner-Institut Berlin, D-1000 Berlin 39, Federal Republic of Germany

D. J. Hinde, J. R. Leigh, J. P. Lestone,* J. O. Newton, J. X. Wei, and S. Elfström†
Department of Nuclear Physics, Research School of Physical Sciences, Australian National University, P.O. Box 4, Canberra, ACT 2601, Australia
(Received 6 September 1991)

Neutrons have been measured in coincidence with fission fragments of the reaction $^{208}Pb(^{16}O,f)$ at bombarding energies ranging between 80 and 130 MeV. Pre-scission and post-scission multiplicities were deduced from the neutron spectra by application of a moving source fit procedure. Particles evaporated before the saddle point configuration of the fissioning nucleus will reduce the nuclear temperature of the transition nucleus. This effect of higher chance fission increases the anisotropies of fission fragment angular distributions compared to the assumption of first chance fission. Compound nuclei with nuclear temperatures considerably smaller than the fission barrier have statistical fission decay times that are much longer than saddle-to-scission times. With these conditions it is plausible that most of the particles evaporated from the fissioning nucleus are emitted before the saddle. Fission fragment angular distributions for $^{208}Pb(^{16}O,f)$ analyzed with the transition state model including the nuclear temperature reduction caused by pre-fission particle emission show "normal" anisotropies at low and near barrier energies.

PACS number(s): 25.85.Ge, 25.70.Gh, 25.70.Jj

I. INTRODUCTION

The fusion process at sub-barrier energies is strongly influenced by couplings of the radial motion to internal nuclear degrees of freedom. The description of this coupling is a challenge for any fusion model designed to understand the amalgamation of two heavy ions and hence to infer all moments of the spin distribution of the compound nucleus. In recent years it has been shown that for systems formed by asymmetric entrance channels the lowest moments of this distribution, the zeroth one (σ_{fus}) and the first one ($\langle l \rangle$), can be reproduced successfully [1–4]. However, going towards symmetric entrance channels, fusion models have more difficulties [5] in giving a consistent description of the reaction mechanism, and independent of the entrance channel asymmetry, large discrepancies have been observed when theoretical values for the second moment ($\langle l^2 \rangle$) were compared with values deduced from the analysis of measured fission fragment angular distributions [6–10]. For instance, Murakami *et al.* [7] extracted a mean-square spin value of 200 for the system $^{208}Pb+^{16}O$ at $E_{lab}=80$ MeV assuming first chance fission. Even sophisticated coupled reaction channel computations [11] carried out for this system underestimated $\langle l^2 \rangle$ roughly by a factor of 2.

Several suggestions have been discussed in the literature to explain those unusually high anisotropies: (a) The effect might be caused by an incorrect assumption employed in present fusion models, where the effective mass used in the quantum mechanical barrier penetration calculation is assumed to be the reduced mass of the system [7]. (b) In heavy systems with relatively low fission barriers a substantial fraction of the partial cross section may undergo precompound fission with incomplete equilibration of the tilting mode [8,10,12]. (c) The statistical transition state model (TSM), comprising only a few collective parameters, might not be adequate to describe the complexity and dynamical aspects of the fission process [13].

This paper addresses another effect which has often been neglected in the interpretation of fission fragment angular distributions using the TSM model. Due to the absence of experimental information on pre-fission particle emission it has been assumed that the nuclear temperature T at the saddle point is that corresponding to first chance fission events. According to the statistical model, the anisotropy A_f of fission fragment angular distributions can be approximately written as

$$A_f=\frac{W(180°)}{W(90°)}\approx 1+\frac{\langle l^2\rangle \hbar^2}{4T\mathcal{J}_{eff}}\ , \tag{1}$$

where $\mathcal{J}_{eff}$ is the effective moment of inertia of the saddle configuration. Of course, T and $\mathcal{J}_{eff}$ will in practice be spin dependent. At bombarding energies close to the Coulomb barrier, where excitation energies of the compound nucleus are often low, the influence of pre-fission particle emission on T can be considerable. At somewhat higher energies these effects were already discussed

*Present address: Los Alamos National Laboratory, Los Alamos, NM 87545.
†Present address: Manne Siegbahn Institute of Physics, 10405, Stockholm, Sweden.

[14,15] for systems with strong competition between neutron evaporation and fission.

Section II gives a short description of the experiment and data analysis. In Sec. III statistical fission decay times calculated by an evaporation code are compared with calculated saddle-to-scission times. The former times are generally much longer, supporting the assumption that most of the neutrons are emitted before the saddle configuration. In Sec. IV calculations of the anisotropy of fission fragment angular distributions are compared with experimental data. A summary is given in Sec. V.

II. EXPERIMENTAL SETUP AND DATA ANALYSIS

The experiment has been performed at the Australian National University (ANU) 14UD Pelletron Accelerator. Self-supporting targets of ^{208}PbS (0.5 and 1.0 mg/cm^2 in thickness, enriched to 99%) were bombarded with ^{16}O beams of energies ranging between 80 and 130 MeV.

A detailed description of the experimental apparatus used has been given by Hinde *et al.* [16] and Ward *et al.* [17]. Here we just give a brief summary of the experimental features. Three solid-state detectors for fission-fragment detection, separated by 90° in azimuthal angle, were placed in the plane perpendicular to the beam at a distance of 15.6 cm from the target position. Coaxial with but 21.5 cm behind each fission detector, cubic NE213 liquid scintillator detectors (size 9.5 cm ×9.5 cm ×9.5 cm) were mounted for neutron detection. The time-of-flight technique was applied for identification of fission fragments and neutrons. In addition, the pulse-shape discrimination technique was used to separate neutrons from γ rays. The relative angles between all the detectors are shown in Table I. The efficiencies of the neutron detectors have been calculated by a Monte Carlo code [18] taking into account the size of the scintillator cell and the distance between its front face and the neutron source.

The neutron time-of flight spectra were transformed into energy spectra using the γ peak as a reference for the time calibration. The light-output signals of the NE213 detectors were calibrated by use of the neutron velocity spectra and three different thresholds were set on the energy signals of the photomultipliers. So, taking advantage of the relative angles between fission and neutron detectors, the detector combinations of Table I together with the threshold settings result in nine sets of three neutron spectra per beam energy. The nine combinations were analyzed separately by a multiple source fit, assuming complete fusion, total kinetic energy values given by

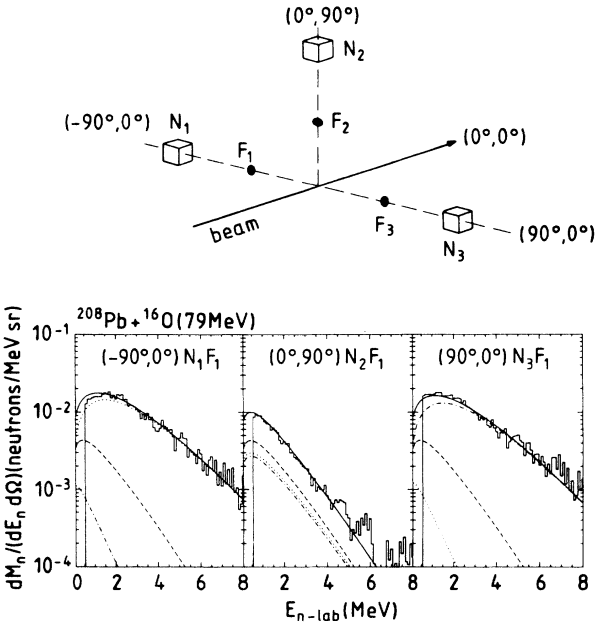

FIG. 1. Sketch of the experimental setup indicating the angle positions for neutron (N_i, $i=1-3$) and fragment (F_i, $i=1-3$) detectors (upper part), and double differential energy spectra of neutrons measured in coincidence with fission fragments of the reaction ^{208}Pb(^{16}O,f) (lower part). The numbers written in parentheses indicate in-plane and out-of-plane positions of the detectors. Results of a multiple source fit analysis for pre-scission, post-scission, and total multiplicity are shown by dashed, dotted and dash-dotted, and solid lines, respectively.

the Viola systematic [19], and a Watt-spectrum shape [20] for pre-scission and post-scission neutron energy spectra. Further, the time resolution of 1.7 ns as observed by the γ peak in the neutron detectors has been included in the fit procedure, and, because gates were set on all fission events, the post-scission neutron multiplicities as well as the post-scission temperature parameters for the two fragment sources in the fit were forced to be equal. A sketch of the detector positions and one out of the nine spectrum combinations for the beam energy of $E_{\rm lab}=78.8$ MeV are shown in Fig. 1. The experimental

TABLE I. Relative angles between fission and neutron detectors.

	F_1	F_2	F_3
N_1	0°	90°	180°
N_2	90°	0°	90°
N_3	180°	90°	0°

TABLE II. Results of multiple source fits. The values given result from nine fits accomplished for each energy and represent the average values with their standard deviations.

$E_{\rm lab}$ (MeV)	$\nu^{\rm pre}$	$\nu^{\rm tot}$	$T^{\rm pre}$ (MeV)	$T^{\rm post}$ (MeV)
77.7	0.9±0.3	3.9±0.5	1.0±0.5	1.15±0.05
78.8	1.4±0.3	4.2±0.2	1.0±0.2	1.01±0.02
82.8	1.5±0.3	4.6±0.1	1.2±0.1	1.04±0.02
88.9	1.9±0.2	5.3±0.2	1.1±0.1	1.05±0.04
99.0	2.4±0.2	6.1±0.1	1.3±0.1	1.11±0.03
114.0	2.8±0.3	6.8±0.1	1.4±0.1	1.18±0.03
128.2	3.4±0.5	7.6±0.2	1.7±0.1	1.17±0.04

neutron energy spectra are displayed by histograms, and the results of the multiple source fit for pre-scission (dashed), post-scission (dotted and dash-dotted), and total (solid) double-differential neutron multiplicities are represented by lines. Table II gives the average values of the fit parameters with standard deviations. The systematic error is estimated to be 10% due to uncertainties in the detection efficiencies and time resolution. Figure 2 shows the deduced ν^{pre} (triangles), ν^{post} (squares), and ν^{total} (circles) as a function of center-of-mass bombarding energy. The solid line represents total neutron multiplicities calculated by an evaporation code with parameters described below. The absolute values of ν^{pre} and their energy dependence are consistent with existing data for similar compound nuclei formed in proton [21] and heavy ion [22] induced reactions.

III. STATISTICAL MODEL CALCULATIONS

Before the experimental pre-scission neutron multiplicities can be used to deduce the temperature at the saddle point, it must be shown that the majority of these neutrons are indeed emitted before the saddle point is reached, and not during the saddle-to-scission transition. To accomplish this, we make use of the statistical model to calculate decay widths, and thus lifetimes. The model assumes statistical equilibrium in the decay of the compound nucleus, and just evaluates the phase space of all decay channels. It does not require any information about reaction dynamics.

The fission decay width $\Gamma_f(E^*,I)$ of a nucleus with excitation energy E^* and spin I may be written as the product of a Bohr-Wheeler factor Γ_f^{BW} and a Kramers factor F_K [23–26] to take into consideration the effect of viscosity in allowing the nucleus to return back over the saddle to the equilibrium region:

$$\Gamma_f(E^*,I)=\Gamma_f^{\text{BW}}(E^*,I)F_K(\beta,\omega_f)\ , \tag{2}$$

with

$$\Gamma_f^{\text{BW}}(E^*,I)=\frac{1}{2\pi\rho(E^*,I)}\int_{-\infty}^{E^*-B_f}\frac{\rho(E^*-B_f-\epsilon,I)d\epsilon}{1+\exp(-2\pi\epsilon/\hbar\omega_f)} \tag{3}$$

and

$$F_K=\sqrt{1+(\beta/2\omega_f)^2}-\frac{\beta}{2\omega_f}\ . \tag{4}$$

Thus Γ_f depends on the nuclear level density ρ, the fission barrier B_f, the nuclear friction constant β, and the frequency ω_f of the inverted oscillator potential which is used to describe the curvature of the nuclear potential at the saddle point. Like Γ_f^{BW}, these parameters also depend on the angular momentum and excitation energy of the compound nucleus, and the calculations are also sensitive to the fusion angular momentum distributions. So, in fact, many parameters are needed to describe, for instance, the ratio of the fission width to the total width Γ (sum over all decay channels), whereas only one experimental value (the ratio of fission to fusion cross section), though often at several energies, is usually used to test the parameter set.

In all computations presented below, it is assumed that the compound nuclei are formed in complete fusion reactions. The angular momentum distributions have been calculated using the barrier fluctuation model [27]. Starting from the frozen density approximation of the Krappe-Nix-Sierk nucleus potential [28], which results in a barrier height of 77.8 MeV, we demonstrate in Fig. 3 that by use of the two additional energy-independent parameters (barrier shift of -3.0 MeV, uniform barrier fluctuation width of ± 2.8 MeV) it is possible to describe the measured fusion cross sections. The resulting mean-squared spin values are much higher than the sharp-cutoff approximation values, but somewhat less than the

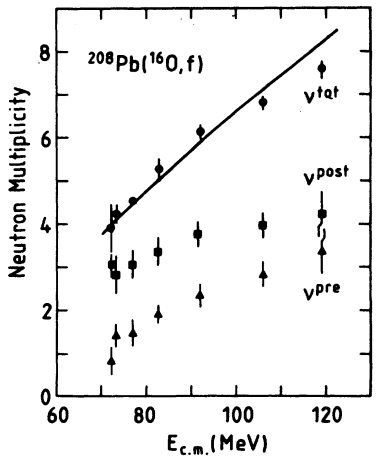

FIG. 2. Pre-scission (triangles), post-scission (squares), and total (dots) neutron multiplicities deduced from the multiple source fits. The line represents the total neutron multiplicities calculated by an evaporation code (see text).

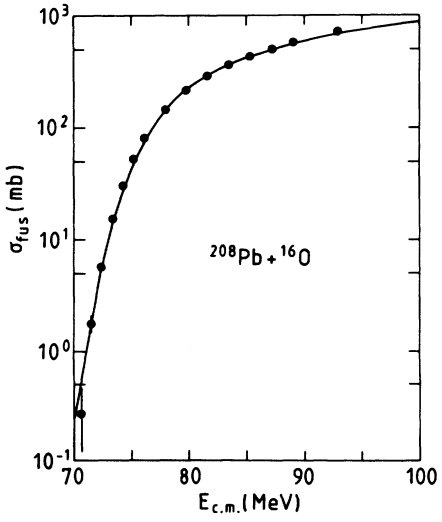

FIG. 3. Fusion excitation function for the system $^{208}\text{Pb}+^{16}\text{O}$ (dots) [34] and the fit of the barrier fluctuation model [27].

values resulting from other calculations. For instance, at $E_{lab}=80$ MeV the sharp-cutoff value is $\langle l^2\rangle=18$, the model of Udagawa *et al.* [29] yields a value of $\langle l^2\rangle=130$, the coupled reaction channel computation of Thompson *et al.* [11] results in $\langle l^2\rangle=107$, while the present barrier fluctuation calculation gives $\langle l^2\rangle=91$.

In the modified Monte Carlo code JULIAN [30,31] the average time for decay at step j in the decay chain is defined by the total decay rate Γ_j of the excited nucleus at step j, and the cumulative lifetime t_i up to step i is given by

$$t_i=\sum_{j=1}^{i}\frac{\hbar}{\Gamma_j}\ . \tag{5}$$

Each emitted particle or fragment can thus be associated with a decay time. As an example, distributions of decay times for multiple chance fission events are plotted in Fig. 4 for two initial temperatures of the compound nucleus ^{224}Th. The calculations were performed using the Sierk barriers B_f [32], a constant Kramers factor F_K of 0.64, and level density ratios a_f/a_n of Ref. [33] with a spin dependence approximated by

$$\frac{a_f}{a_n}(I)=\left[\frac{a_f}{a_n}(I=0)-1\right]\left[\frac{B_f(I)}{B_f(I=0)}\right]^{1/4}+1\ . \tag{6}$$

This parameter set reproduces the measured ratios [34] of evaporation residue cross sections and fusion cross sections and is used throughout this section.

Calculations for intermediate initial temperatures (bombarding energies) were also performed, and the locus of decay times for multiple chance fission ($i=1-6$) are shown in Fig. 5, corresponding to pre-fission neutron multiplicities of zero to five. The use of a_f/a_n values closer to unity would result in longer times for early chances. Neutron emission that occurs in competition with, or during the fission process up to and including the saddle point, will be effective in reducing the temperature at the saddle point used in the calculation of fission fragment angular distributions, while those emitted after the saddle will not. Extrapolation of calculations [35] of saddle-to-scission times to finite angular momenta [36] allows estimates of $\approx 3\times10^{-21}$ s for two-body viscosity, or

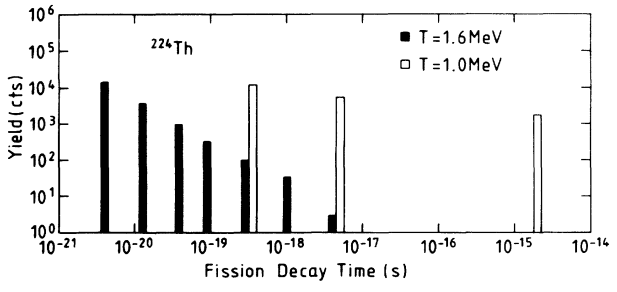

FIG. 4. Statistical model predictions of distributions of decay times for multiple chance fission events of the compound nucleus ^{224}Th. Results for a nuclear temperature T of $T=1.0$ MeV are shown by open bars and those for $T=1.6$ MeV by solid bars.

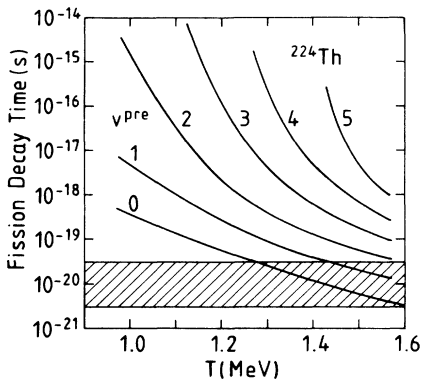

FIG. 5. Nuclear temperature dependence of statistical decay times for multiple chance fission ($i=1-6$) of the compound nucleus ^{224}Th, corresponding to pre-fission neutron multiplicities of $\nu^{pre}=0-5$. The hatched band shows the range of theoretical saddle-to-scission times.

$\approx 3\times10^{-20}$ s for one-body viscosity, to be made for this compound nucleus. This region is shown by the diagonally hatched band in Fig. 5.

The experimental ν^{pre} values will correspond to an unknown distribution of chances, however, for our purposes the actual distribution is irrelevant, since even for first chance fission ($i=1$, $\nu^{pre}=0$) the decay time is above the saddle-to-scission band up to $T\approx1.3$ MeV ($E_{c.m.}\approx92$ MeV), while for $\nu^{pre}=1$, this is true up to $T\approx1.4$ MeV ($E_{c.m.}\approx106$ MeV). Experimentally, $\nu^{pre}\geq1$, thus the saddle-to-scission time should be negligible compared to the pre-saddle time at least up to $T\approx1.3$ MeV, and thus we can be confident that the pre-scission neutrons observed can be used to determine the temperature at the saddle point. At higher initial temperatures (bombarding energies), this procedure may underestimate the saddle temperature due to the greater likelihood of neutron emission during the saddle-to-scission transition.

In the following section we will, however, assume that all observed neutrons are effective in reducing the saddle temperature at all energies.

IV. ANALYSIS OF FISSION FRAGMENT ANGULAR DISTRIBUTIONS

The relative cross section $W(E^*,\theta)$ for fission fragments emitted from compound nuclei with total excitation energies E^*, with directions of spin I perpendicular to the beam axis and with scattering angles θ, is expressed within the statistical model as

$$W(E^*,\theta)\propto\sum_{I,K}P_I[\Gamma_f(E^*,I,K)/\Gamma(E^*,I)](I+\tfrac{1}{2})\times|D^I_{M=0,K}(\theta)|^2\ . \tag{7}$$

The angular distribution thus depends on the weight factor P_I which is usually set equal to the partial fusion cross section, on the fission probability $\Gamma_f(E^*,I,K)/\Gamma(E^*,I)$ for a nuclear state with projection

K onto the nuclear symmetry axis, and on the rigid-rotor functions $D^I_{M,K}$. The fission probability for state (E^*,I,K) may be rewritten as product of the partial fission probability and the relative fission decay width:

$$\Gamma_f(E^*,I,K)/\Gamma(E^*,I) = [\Gamma_f(E^*,I,K)/\Gamma_f(E^*,I)][\Gamma_f(E^*,I)/\Gamma(E^*,I)] , \quad (8)$$

where $\Gamma_f(E^*,I)=\sum_K \Gamma_f(E^*,I,K)$, and $\Gamma(E^*,I)$ is the total decay width of the nuclear level (E^*,I). The relative fission decay width is set to one for compound nucleus levels that undergo fission, and a Gaussian distribution is assumed for $\Gamma_f(E^*,I,K)$ with variance $K_0^2=\mathcal{J}_{\rm eff}T/\hbar^2$ which is defined by the effective moment of inertia $\mathcal{J}_{\rm eff}$ and the nuclear temperature T of the transition state nucleus. The computations were performed using the spin-dependent moments of inertia and fission barriers of Sierk [32], the approximation of the K dependence of the barriers [37] as described in Ref. [15], and the level density parameter a_f of Sec. III.

Pre-fission particle evaporation will modify the spin population of the compound nucleus (P_I) and the saddle-point temperatures (T_I). These modifications are expected to depend on the angular momentum of the compound nucleus, and thus are considered for each spin I in Eq. (7). We use the evaporation code JULIAN to extract population and excitation energies of all compound nucleus levels after evaporation of $\nu^{\rm pre}$ neutrons. In Fig. 6 the spin dependence of P_I and T_I before and after pre-fission particle evaporation is shown for $K=0$ and $E_{\rm c.m.}=73$ MeV. The nuclear temperature at angular momentum I has been computed by

$$T_I=\{[E^*-B_f(I,K=0)-E_{\rm rot}(I,K=0) -E_p(I)]/a_f(I)\}^{1/2} , \quad (9)$$

where $E_{\rm rot}$ is the rotational energy of the compound nucleus and E_p the energy taken away by evaporated particles. It is demonstrated that at low excitation energies pre-fission particle evaporation causes moderate modifications of the spin population but significant reduction of the nuclear temperature of the transition state nucleus.

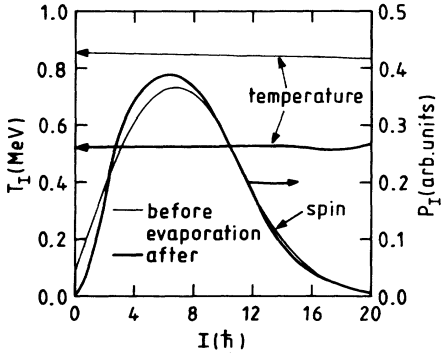

FIG. 6. Nuclear temperatures T_I and spin distributions P_I of the compound nucleus ^{224}Th before (thin lines) and after (thick lines) pre-fission particle evaporation. The computations were performed for the fusion-fission reaction of ^{208}Pb(^{16}O,f) at $E_{\rm lab}=78.8$ MeV.

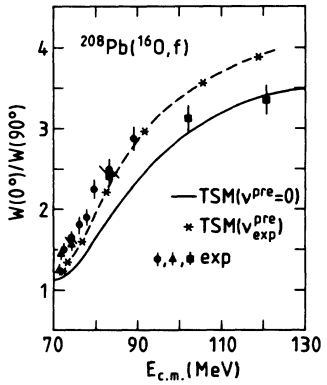

FIG. 7. Calculated and measured fission fragment anisotropies. Experimental values are plotted by solid symbols. The solid line represents the prediction of the transition state model assuming first chance fission. With the assumption that all experimental pre-scission neutrons are emitted before or at the saddle point, the model yields the values displayed by stars. The dashed line is drawn to guide the eye.

Finally the effect of pre-fission particle evaporation on calculated fission-fragment angular distributions for the energy range of 70 MeV $\leq E_{\rm c.m.} \leq$ 130 MeV is shown in Fig. 7. Anisotropies measured by several groups [7,34,38] are plotted by solid symbols and are compared to TSM calculations. Computations with the assumption of first chance fission are represented by the solid line. Consideration of pre-fission particle emission with neutron multiplicities $\nu^{\rm pre}$ of Table II increases the anisotropies to values which are indicated by stars. The dashed line is drawn to guide the eye.

The assumption that all particles emitted by the fissioning nucleus are evaporated before or at the saddle gives good agreement at low excitation energies (near barrier bombarding energies) but is contradicted by the anisotropies at higher energies, where the nuclear temperature can be sufficiently high to emit neutrons also on the way from saddle to scission, as was indicated in the calculations shown in Fig. 5. Thus if we could determine the excitation function for $\nu^{\rm pre}$ in the absence of dynamical effects (as in a pure statistical model calculation), it may be that the deviation of the true $\nu^{\rm pre}$ from these values would occur rather near in energy to the deviation of the calculated anisotropy from that measured.

V. SUMMARY

Up to now many attempts have failed to describe the anisotropies of fission fragment angular distributions measured at energies close to the fusion barrier. In this paper we show that the assumption of first chance fission often used in the analysis of fission fragment angular dis-

tributions is not correct. For the reaction ^{208}Pb(^{16}O,f) pre-fission particle emission causes considerable reduction of the nuclear temperature of the compound nucleus and a slight modification of its spin distribution. When these effects were taken into account, a satisfying description of fragment angular distributions was achieved for near barrier bombarding energies by application of the transition state model, and by use of a fusion angular momentum distribution consistent with fitting the excitation function. There seems to be no evidence for anomalous anisotropies.

Our interpretations of measured pre-scission neutron multiplicities and fission fragment angular distributions are based on the validity of applying the statistical model to these reactions. For several nuclear systems this model has been able to reproduce measured neutron multiplicities at moderate excitation energies [36], where the nuclear temperature is smaller than the fission barrier, and where statistical fission decay times are longer than the times related to fission dynamics, such as transient delay times and saddle-to-scission times. However, as stated in Ref. [36], even at low bombarding energies reliable parameter sets for statistical model calculations are not available yet. For instance, with $a_n = a_f = A/10$, Sierk's fission barriers, and $F_K = 1$, the value for ν^{pre} is reproduced at $E_{\text{lab}} = 77.7$ MeV, but is underestimated by a factor of 2 for the next two energies and is underestimated even more at higher energies. Such disagreement might be attributed to dynamical effects, shell effects, collective enhancement of the level density at the saddle point, and the effect of temperature on the above. Thus at this stage, calculations cannot be reliably used as a replacement of measured pre-scission neutron multiplicities.

To improve the understanding of fission it is necessary to continue with systematic measurements of fusion cross sections, fission fragment angular distributions, and pre-scission particle emission. With better data it may even be possible to estimate the pre-saddle and post-saddle particle multiplicities and thus the saddle point temperature.

One of us (H.R.) is indebted to the nuclear physics group at ANU for their kind hospitality and support during his visit when part of this work was done.

[1] S. Gil, R. Vandenbosch, A. J. Lazzarini, D.-K. Lock, and A. Ray, Phys. Rev. C **31**, 1752 (1985).
[2] S. Gil, D. Abriola, D. E. DiGregorio, M. di Tada, M. Elgue, A. Etchegoyen, M. C. Etchegoyen, J. Fernández Niello, A. M. J. Ferrero, A. O. Macchiavelli, A. J. Pacheco, J. E. Testoni, P. Silveira Gomes, V. R. Vanin, A. Charlop, A. García, S. Kailas, S. J. Luke, E. Renshaw, and R. Vandenbosch, Phys. Rev. Lett. **65**, 3100 (1990).
[3] S. Gil, R. Vandenbosch, A. Charlop, A. García, D. D. Leach, S. J. Luke, and S. Kailas, Phys. Rev. C **43**, 701 (1991).
[4] R. G. Stokstad, D. E. DiGregorio, K. T. Lesko, B. A. Harmon, E. B. Norman, J. Pouliot, and Y. D. Chan, Phys. Rev. Lett. **62**, 399 (1989).
[5] M. L. Halbert, J. R. Beene, D. C. Hensley, K. Honkanen, T. M. Semkow, V. Abenante, D. G. Sarantites, and Z. Li. Phys. Rev. C **40**, 2558 (1989).
[6] R. Vandenbosch, T. Murakami, C.-C. Sahm, D. D. Leach, A. Ray, and M. J. Murphy, Phys. Rev. Lett. **56**, 1234 (1986).
[7] T. Murakami, C.-C. Sahm, R. Vandenbosch, D. D. Leach, A. Ray, and M. J. Murphy, Phys. Rev. C **34**, 1353 (1986).
[8] H. Rossner, J. Erxmeyer, D. Hilscher, and M. Lehmann, in *Proceedings of the Symposium on Heavy Ion Interactions Around the Coulomb Barrier, Legnaro, Italy, 1988,* edited by C. Signorini, S. Skorka, P. Spolaore, and A. Vitturi, Lecture Notes in Physics Vol. 317 (Springer, Berlin, 1988), p. 167.
[9] Huanqiao Zhang, Jincheng Xu, Zuhua Liu, Jun Lu, Kan Xu, and Ming Ruan, Phys. Lett. B **218**, 133 (1989).
[10] V. S. Ramamurthy, S. S. Kapoor, R. K. Choudhury, A. Saxena, D. M. Nadkarni, A. K. Mohanty, B. K. Nayak, S. V. Sastry, S. Kailas, A. Chatterjee, P. Singh, and A. Navin, Phys. Rev. Lett. **65**, 25 (1990).
[11] I. J. Thompson, M. A. Nagarajan, J. S. Lilley, and M. J. Smithson, Nucl. Phys. **A505**, 84 (1989).
[12] V. S. Ramamurthy and S. S. Kapoor, Phys. Rev. Lett. **54**, 178 (1985); Phys. Rev. C **32**, 2182 (1985).
[13] P. Fröbrich and J. Marten, Z. Phys. A **339**, 171 (1991).
[14] H. Rossner, D. Hilscher, E. Holub, G. Ingold, U. Jahnke, H. Orf, J. R. Huizenga, J. R. Birkelund, W. U. Schröder, and W. W. Wilcke, Phys. Rev. C **27**, 2666 (1983).
[15] H. Rossner, J. R. Huizenga, and W. U. Schröder, Phys. Rev. C **33**, 560 (1986).
[16] D. J. Hinde, J. R. Leigh, J. J. M. Bokhorst, J. O. Newton, R. L. Walsh, and J. W. Boldeman, Nucl. Phys. **A472**, 318 (1987).
[17] D. Ward, R. J. Charity, D. J. Hinde, J. R. Leigh, and J. O. Newton, Nucl. Phys. **A403**, 189 (1983).
[18] R. A. Cecil, B. D. Anderson, and R. Madey, Nucl. Instrum. Methods **161**, 439 (1979).
[19] V. E. Viola, K. Kwiatkowski, and M. Walker, Phys. Rev. C **31**, 1550 (1985).
[20] B. E. Watt, Phys. Rev. **87**, 1037 (1952).
[21] M. Strecker, R. Wien, P. Plischke, and W. Scobel, Phys. Rev. C **41**, 2172 (1990).
[22] D. J. Hinde, H. Ogata, M. Tanaka, T. Shimoda, N. Takahashi, A. Shinohara, S. Wakamatsu, K. Katori, and H. Okamura, Phys. Rev. C **39**, 2268 (1989).
[23] P. Grangé and H. A. Weidenmüller, Phys. Lett. **96B**, 26 (1980).
[24] P. Grangé, Li Jun-Qing, and H. A. Weidenmüller, Phys. Rev. C **27**, 2063 (1983).
[25] P. Grangé, S. Hassani, H. A. Weidenmüller, A. Gavron, J. R. Nix, and A. J. Sierk, Phys. Rev. C **34**, 209 (1986).
[26] A. Gavron, A. Gayer, J. Boissevain, H. C. Britt, T. C. Awes, J. R. Beene, B. Cheynis, D. Drain, R. L. Ferguson, F. E. Obenshain, F. Plasil, G. R. Young, G. A. Petitt, and C. Butler, Phys. Rev. C **35**, 579 (1987).
[27] H. J. Krappe, K. Möhring, M. C. Nemes, and H. Rossner, Z. Phys. A **314**, 23 (1983).
[28] H. J. Krappe, J. R. Nix, and A. J. Sierk, Phys. Rev. C **20**,

992 (1979).
[29] T. Udagawa, B. T. Kim, and T. Tamura, Phys. Rev. C **32**, 124 (1985).
[30] M. Hilman and Y. Eyal (unpublished).
[31] H. Rossner, D. Hilscher, D. J. Hinde, B. Gebauer, M. Lehmann, M. Wilpert, and E. Mordhorst, Phys. Rev. C **40**, 2629 (1989).
[32] A. J. Sierk, Phys. Rev. C **33**, 2039 (1986).
[33] J. Tōke and W. J. Swiatecki, Nucl. Phys. **A372**, 141 (1981).
[34] E. Vulgaris, L. Grodzins, S. G. Steadman, and R. Ledoux, Phys. Rev. C **33**, 2017 (1986).
[35] N. Cârjan, A. J. Sierk, and J. R. Nix, Nucl. Phys. **A452**, 381 (1986).
[36] J. O. Newton, D. J. Hinde, R. J. Charity, J. R. Leigh, J. J. M. Bokhorst, A. Chatterjee, G. S. Foote, and S. Ogaza, Nucl. Phys. **A483**, 126 (1988).
[37] M. Prakash, V. S. Ramamurthy, S. S. Kapoor, and J. M. Alexander, Phys. Rev. Lett. **52**, 990 (1984).
[38] B. B. Back, R. R. Betts, J. E. Gindler, B. D. Wilkins, S. Saini, M. B. Tsang, C. K. Gelbke, W. G. Lynch, M. A. McMahan, and P. A. Baisden, Phys. Rev. C **32**, 195 (1985).